Morphological, secondary metabolite and ITS (rDNA) variability within usnic acid containing lichen thalli of the genus Xanthoparmelia explored at the local scale of rock outcrop in Western Italian Alps

Matteucci, Enrica; Occhipinti, Andrea; Piervittori, Rosanna; Maffei, Massimo E; Favero-Longo, Sergio E. Morphological, secondary metabolite and ITS (rDNA) variability within usnic acid containing lichen thalli of the genus Xanthoparmelia explored at the local scale of rock outcrop in Western Italian Alps. CHEMISTRY & BIODIVERSITY. None pp: 1-27.
DOI: 10.1002/cbdv.201600483

Morphological, secondary metabolite and ITS (rDNA) variability within usnic acid-containing lichen thalli of *Xanthoparmelia* explored at the local scale of rock outcrop in W-Alps

Enrica Matteucci,[a] Andrea Occhipinti,[b] Rosanna Piervittori,[a] Massimo E. Maffei,[b] Sergio E. Favero-Longo*,[a]

[a] Unità di Lichenologia, Dipartimento di Scienze della Vita e Biologia dei Sistemi, Università degli Studi di Torino, Viale Mattioli 25, 10125, Torino, Italia, sergio.favero@unito.it

[b] Unità di Fisiologia Vegetale, Dipartimento di Scienze della Vita e Biologia dei Sistemi, Università degli Studi di Torino, Via Quarello 15/A, 10135, Torino, Italia

Lichen secondary metabolites (LSMs) are regarded with interest for valuable biological properties, but chemical variability among/within lichen *taxa* has been only fragmentarily characterized by advanced analytical techniques. Knowledge of variability at a local geographic scale has been particularly neglected, while it should address the collection of chemically homogeneous materials to test and exploit LSMs. Here we evaluated the chemical variability of 48 *Xanthoparmelia* specimens from two rock outcrops in Western Italian Alps, representative of nine morphotypes and sixteen rDNA ITS haplotypes. Qualitative and quantitative analyses were performed by HPLC-DAD-ESI-MS_2 and UPLC-HDR-DAD, respectively, and revealed the occurrence of 18 LSMs. Chemical partition allowed distinguishing six chemical groups, only partially overlapping with distinct morphotypes and three divergent haplotype groups, which, overall, accounted for the co-occurrence of different *taxa* only in part identifiable with species described for Europe. Some morphotypes were variable in presence and concentration of LSMs, and chemical divergences also characterized single ITS haplotypes. Accordingly, the collection of chemically homogeneous materials, even at a local scale, may be not properly addressed by morphological features and ITS barcoding, and should be confirmed by a specimen-level chemical characterization.

Keywords: natural products ● phytochemistry ● depsidones ● liquid chromatography and mass spectrometry techniques ● ITS-rDNA barcoding

Introduction

Since the dawn of lichenology, chemical discrimination has been roughly used for lichen classification and more than 1000 lichen secondary metabolites (LSMs) have been described so far [1][2]. The necessity to better characterize lichen chemical patterns has been renewed by the interest to exploit untapped biological properties of LSMs, in particular for pharmaceutical applications [3-7].

Lichen chemical variability depends on either the difference of metabolite concentrations and replacements with related metabolites (same "chemosyndrome") or biogenetically distinct metabolites (different "chemosyndrome") [8]. Advanced chromatography and mass spectrometry techniques strongly contribute to improve knowledge on LSMs [9-12]; however, the qualitative and quantitative accuracy of these techniques has been marginally exploited to assess the chemical variability among/within circumscribed lichen *taxa* [13-16].

Studies on the chemotaxonomical significance of LSMs [17][18], and even studies on the biological effects of LSMs crude extracts [19][20], have been often based on the use of traditional analytical techniques with low specificity and sensitivity, such as TLC, which generate contrasting reports regarding the presence/absence of LSMs [21] and do not allow accurate quantitative comparisons of compound concentrations [8][22]. Instead, only a reliable knowledge on the chemical variability of a *taxon* in terms of presence and concentrations of LSMs, including trace compounds, may clarify potential and difficulties in testing and exploiting its extracts [6][7][22].

Lichens of the world-wide distributed genus *Xanthoparmelia* (VAINIO) HALE are known to synthetize more than 90 LSMs [23]. Some of these show antioxidant [24] and cancer-chemopreventive activity [25], as well as UV screening capacity [26], defence functions against herbivores [27] and toxic effects to domestic and wild mammals [28]. Crude extracts from *X. chlorochroa* (TUCKERMAN) HALE exhibited antiproliferative effects against lymphoma (Rajii) cells [19]. Although *Xanthoparmelia* lichens may thus appear a promising source of natural products, they may also pose difficulties and limitations for the collection of homogeneous materials in bulk quantities to test and exploit LSMs [22]: the high LSMs availability lies within a complex framework of variability, which is still widely unresolved.

More than 400 *Xanthoparmelia* species had been described on the basis of morphological and chemical characters [23][29][30]. The number of species even exceeded 750 upon the use of molecular markers for phylogenetic reconstructions, because of the synonymization of some related genera [31]

and the recognition of cryptic species (*i.e.* sharing the same phenotype, but phylogenetically distinct; *e.g.* [32]). However, early molecular studies showed that genetic distances between species (excluding those previously included in separate genera) are low (<0.015 substitutions per site, s/s, for ITS sequences, the official barcoding marker for Fungi [33]), if compared with interspecific distances in other parmelioid genera [34]. More recently, the *Xanthoparmelia* diversity at the continental (western North America) and regional (*e.g.* South Korea) scale revealed considerable discrepancy between traditionally circumscribed species and phylogenetic evidences [17][18][30]. Genetically distinct clusters included multiple traditional species, based on morphology and/or chemistry, and at the same time the most common morphological/chemical species were distributed in different phylogenetic clusters [18]. A relatively low number of *Xanthoparmelia* species (n=34) has been reported in Europe [35][36], where the detection of new chemotypes is still often signalled [37] and extensive phylogenetic analyses are still to be conducted (list and phenotypic characters of European species in *Table S1* in the Supporting Information). In the complex framework of variability of *Xanthoparmelia*, partially surveyed over large geographic scale, a clear demarcation between inter- and intraspecific phenotypic (morphological and chemical) variation may be thus widely questionable, and a high morphological and chemical variation appears common for many species-level genetic groups [38].

The complicated patterns of *Xanthoparmelia* variability even received minor attention at the scale of rock outcrop, where the possibility of recognizing chemically homogeneous thalli on the basis of morphology and/or barcoding may be crucial to test and exploit their LSMs. Sympatry/overlapping distributions of *Xanthoparmelia* species have been frequently noted [39] and predicted along gradients of macro- and micro-environmental factors [40], but both inter- and intra-specific patterns of variability at the local scale have not been experimentally screened and discussed with reference to advanced chemical characterizations or molecular markers.

In this work, we characterized what chemical variability was associated to distinct morphotypes and genotypes of *Xanthoparmelia* on two rock outcrops (ca. 50×50 m), 60 km apart but similar for (micro-)climate conditions, in Western Italian Alps. We aimed to examine at the local scale of rock outcrop (**I**) whether presence and/or concentration ranges of LSMs were steady for a certain morphotype, and how the observed morpho-chemical variability fitted the available phenotype descriptions of *Xanthopamelia* species, (**II**) whether distinct morpho-chemical phenotypes reflected the haplotype variability of the ITS barcode and how their sequences were inserted in an ITS-based *Xanthoparmelia* phylogeny. With these aims, we surveyed *Xanthoparmelia* morphological diversity with reference to traits traditionally used to define the species boundaries (including thallus adnation, lobation, lower surface colour and occurrence of isidia as reproductive structures [23]). A qualitative and quantitative analysis of LSMs in thalli representative of the morphotype diversity recognized at each outcrop was performed by HPLC-DAD-ESI-MS_2 and UPLC-HDR-DAD, respectively. The haplotype variability of the ITS barcode was considered to evaluate the relationship between morpho-chemical and genotypic variability.

Results and Discussion

Morphological variability

Yellow-green thalli of *Xanthoparmelia*, which owe their colour to usnic acid in the upper cortex [23], covered av. 50% of both the rock outcrops, appearing the dominant component of lichen vegetation. On outcrop 1, six non-isidiate morphotypes were distinguished with reference to thallus adnation, lobation and lower surface colour (M-I/M-VI) (*Table 1*). Four of them (M-II, M-IV/M-VI) were also abundantly observed on outcrop 2, where 3 additional isidiate morphotypes (M-VII/M-IX), sharing the co-occurrence of isidia from (sub-)globose to cylindrical and branched, subordinately occurred. All non-isidiate morphotypes, with one exception (M-III), were compatible with a group of species reported for Italy, which share the same wide range of morphological variability (lower surface colour of thalli from dark to pale brown, loosely to tightly adnate thalli, subirregular to sublinear lobes), but have been distinguished, as "chemical strains" (*sensu* [41]), by the occurrence of different medullary LSMs (*Chemical formulae 1*): salazinic (**5**) and consalazinic (**1**) acids in *X. sublaevis* (Cout.) Hale, fumarprotocetraric acid (**14**) in *X. protomatrae* (Gyeln.) Hale, and stictic (**10**), constictic (**2**) and norstictic (**13**) acids in *X. cumberlandia* (Gyeln.) Hale [23][42][43]. However, the presence in Europe of this latter species, primarily reported in North America, has been questioned and the need of confirmation by molecular data has been suggested [35] [36]. The non-isidiate morphotype M-III, macroscopically distinguished by the sublinear to laciniate lobes was compatible with *X. stenophylla* (Ach.) Ahti & D. Hawksw., a species widely reported in Europe (and in Italy), chemically characterized by the presence of salazinic (**5**), consalazinic (**1**) and, occasionally, lobaric acids in the medulla [42] [chemical formulae of LSMs not detected in the examined sample set, as lobaric acid, are available in [44][45]].

The sub-globose to cylindrical shape of isidia and the other morphological characters of the isidiate thalli were compatible with *X. conspersa* (Ehrh. ex Ach.) Hale, a worldwide common pantemperate species, characterized by the presence in the medulla of stictic acid (**10**) and related LSMs as constictic (**2**), cryptostictic (**9**), norstictic (**13**) acids, with traces of menegazziaic (**11**) and hyposalazinic acids having been also reported.

Brown thalli of *Xanthoparmelia*, with melanoid substances in the upper cortex, subordinately occurred on the two outcrops (cover values <5%) and were not considered in the study of morpho-chemical and phylogenetic variability.

Characterization of Xanthoparmelia *chemical variability by HPLC-DAD-ESI-MS$_2$ and UPLC-HDR-DAD*

Qualitative and quantitative chemical analyses were performed on 24 specimens from each of the two rock outcrops. Each specimen set included adult thalli representative and quantitatively proportional to the local abundance of morphotypes M-I/M-IX (*Table 1*), and clearly recognizable as distinct foliose rosettes. The qualitative analyses revealed the occurrence of 18 LSMs (**1-18**) that were characterized based on UV-Vis absorption and MS fragmentation spectra (*Table 2*). Beside the cortical dibenzofuran-derivative usnic acid (**18**), β-orcinol depsidones reported in literature as medullary LSMs in yellow-green Xanthoparmelias [23], including consalazinic (**1**), constictic (**2**), protocetraric (**3**), connorstictic (**4**), salazinic (**5**), peristictic (**6**), conprotocetraric (**7**), substictic (**8**), cryptostictic (**9**), stictic (**10**), menegazziaic (**11**), norstictic (**13**), fumarprotocetraric (**14**), and methylhypoprotocetraric (**17**) acids, were detected (*Chemical formulae 1*). We also found three unidentified compounds [quasi-molecular ions $[M-H]^{-1}$: 403 (**12**), 427 (**15**) and 359 (**16**), *m/z*; fragmentation pathways in *Fig. S1* in the Supporting Information], unlisted in LSMs catalogues [44][45]. Their characterization was beyond the aim of this work, which was focused on the variability of LSMs patterns at the local scale.

The detected range of concentrations for each metabolite was operationally examined with reference to three arbitrarily defined concentration categories: highly-concentrated (>600 μg g^{-1} dry wt; HC), low-concentrated (25< μg g^{-1} dry wt <600; LC) and trace (<25 μg g^{-1} dry wt) amounts (*Table 2*). Throughout the specimen set, quantitative analyses showed that usnic acid (**18**) was the most abundant compound (av. 2.4 mg g^{-1} dry wt), as expected for yellow-green Xanthoparmelias [23]. Moreover, UPLC-HDR-DAD analyses highlighted a significant variability in the occurrence and content of depsidones and unidentified LSMs (*Table 2*). To accomplish research objective **I**, we considered such patterns of variability with regard to (a) their correlation with the recognized morphotypes, (b) the different ranges of LSMs contents and the possibility, at the local level, of utilizing the presence/absence of LSMs, as a reliable criterion for the taxonomic treatment of *Xanthoparmelia*, as traditionally proposed in identification keys, and (c) their congruency with expected LSMs contents in European and non-European species compatible with the observed morphotypes.

(a) *Fig. 1* shows the overall metabolite variability displayed by Principal Coordinate Analysis (PCoA), and its relationship with the recognized morphotypes at the two rock outcrops. The first principal coordinate separates salazinic acid (**5**) from all other compounds by negative values, whereas menegazziaic acid (**11**) is separated by positive values. Constictic (**2**), cryptostictic (**9**) and stictic (**10**) acids are discriminated by positive values of the second principal coordinate. A cluster analysis (UPGMA) based on the quantified chemical contents (*Table 2*) divided six groups/chemotypes (**i-vi**; *Fig. 1* and *Fig. S2* in the Supporting Information), which were identified with reference to the HC compounds as follows: (**i**; n=3) stictic (**10**), cryptostictic (**9**), constictic (**2**), norstictic (**13**) acids; (**ii**; n=4) salazinic (**5**), cryptostictic (**9**), stictic (**10**), constictic (**2**), norstictic (**13**) acids; (**iii**; n=1) stictic (**10**), constictic (**2**), norstictic (**13**), menegazziaic (**11**) acids; (**iv**; n=11) menegazziaic acid (**11**); (**v**; n=25) salazinic (**5**) and norstictic (**13**) acids; (**vi**; n=4) chemically intermediate between the **iv** and **v** groups, containing salazinic (**5**), norstictic (**13**) acids, but also menegazziaic acid (**11**).

Chemotype groups **i**-**iii** corresponded to the isidiate morphotypes M-VII/M-IX from outcrop 2, while chemotypes **iv**-**vi** included all the non-isidiate morphotypes (M-I/M-VI) from both the outcrops. Beyond this main separation of morpho-chemotypes [between isidiate thalli, characterized by the stictic (**10**) -constictic (**2**) -cryptostictic (**9**) chemosyndrome, and non-isidiate thalli, with variable contents of salazinic (**5**) and menegazziaic (**11**) acids], any secondary correlation between the other morphological characters and the different chemotypes was detected. All the chemotypes associated to the non-isidiate morphotypes were found on both the outcrops, although a prevalence for chemotypes **v** and **iv** on outcrops 1 and 2, respectively, was recognizable.

(b) Most of the depsidones displayed wide concentration ranges and were assignable to at least two of the three concentration categories (*Table 2* and *Table S2* in the Supporting Information). Salazinic acid (**5**) was steadily present, occurring as HC compound or in traces. Such generalized production of salazinic acid (**5**) in the whole specimen set was unexpected, as trace contents were not recognizable with traditional analytical techniques such as TLC because of lower sensitivity. This finding is worth of consideration with regard to the usage of the salazinic acid presence/absence as a taxonomic criterion in the treatment of *Xanthoparmelia* [23][42], but also with regard to the definition of incongruencies between chemical and phylogenetic results, when these are based on TLC analyses [17][18]. Constictic (**2**), cryptostictic (**9**) and stictic (**10**) acids mostly co-occurred as HC compounds or were absent. This fact and their consistent association with the isidiate thalli make their presence/absence, at least in the examined context, a more reliable criterion of distinctiveness. The relative concentrations of the three metabolites appeared variable, and possibly related to those of salazinic acid (**5**): concentrations of cryptostictic acid (**9**) higher than those of stictic acid (**10**) characterized specimens which also contained salazinic acid (**5**) as HC compound; on the other hand, a stictic (**10**)/cryptostictic (**9**) acids ratio >1.5 was found in specimens with salazinic acid (**5**) in traces. Norstictic acid (**13**), which mostly co-occurred in high concentrations with these metabolites, was absent in samples containing menegazziaic acid (**11**), with one exception. Menegazziaic acid (**11**) displayed a continuous range of concentrations, occurring as HC, LC or trace compound or being absent.

On the whole, LSMs which occurred as HC compounds in some of the thalli mostly displayed wide concentration ranges when considered through the whole set of specimens, suggesting some difficulty to univocally recognize a taxonomic significance to the LSMs presence/absence criterion.

Other LSMs, accumulated at low and/or trace quantities, were consistently associated to the different HC compounds (*Fig. 1*; *Table S2* in the Supporting Information), with the exception of an unidentified compound with $[M-H]^-$ 427 *m/z* (**15**), occurring in all, out of one, of the examined thalli (*Table 2*). The detected protocetraric (**3**) and conprotocetraric (**7**) acids, unreported and scanty observed in *Xanthoparmelia* in Europe, respectively [35], could not be observed by TLC (data not shown). This confirms that traditional analytical techniques, which are still often used to characterize crude extracts [17][19],

might not provide an accurate metabolic profile and the detection of LC and trace compounds with potential biological activities [6][7]: antioxidant, antimicrobial and cytotoxic activities were indeed shown for protocetraric acid (**3**) [4][5].

(c) The isidiate morphotypes M-VII/IX characterized by the stictic (**10**) -constictic (**2**) -cryptostictic (**9**) chemosyndrome may be recognized as *X. conspersa*. However, they did not exhibit the production of menegazziaic (**11**) and hyposalazinic acids, which may be found in this species [23]. Moreover, all the isidiate thalli were shown to produce salazinic acid (**5**), as HC or trace compound, which is not expected in the species, while it is secreted by *X. tinctina* (MAHEU & A. GILLET) HALE, another isidiate species, widely reported in Europe and in Italy. However, *X. tinctina* does not show the stictic chemosyndrome and is also morphologically distinguished by a different shape of isidia [23]. The combination of stictic (**10**), salazinic (**5**), constictic (**2**), cryptostictic (**9**) and norstictic (**13**) acids is unreported for Europe in both isidiate and non-isidiate morphotypes, and uniquely reported for the isidiate *X. succedans* ELIX AND JOHNSTON in Australia and Brazil [23] (phenotypic characters of non-European species considered in this section are listed in *Table S3* in the Supporting Information). This species shows adnation and lobation characters congruent with the observed morphotypes, but a brown colour of the lower cortex, which, instead, was mostly black in the examined samples, as described in *X. conspersa* and *X. tinctina*.
The non-isidiate thalli similarly displayed unreported LSMs associations. The production of salazinic acid (**5**) as HC compound by chemotype **v**, and the associated morphological characters of thalli, may be compatible with *X. sublaevis*. However this species is not expected to produce norstictic acid (**13**). The production of salazinic (**5**) and norstictic acid (**13**) was reported in several non-isidiate species from the Southern Hemisphere and North America [23]: some of these species also produce protocetraric acid (**3**), which we detected as LC or trace compounds, and show a high, but not complete, congruency with the observed morphological characters (*Table S3* in the Supporting Information).
The production of menegazziaic acid by *Xanthoparmelia* is only reported in association to stictic acid and related compounds, in isidiate European species as *X. conspersa* (as traces) and *X. verrucigera* (NYL.) HALE, and in the Southern Hemisphere in *X. mougeotina* (NYL.) GALLOWAY and *X. congensis* (B. STEIN) HALE [23]. On the basis of a traditional approach of species description, non-isidiate morphotypes M-II and M-IV/M-VI, characterized by menegazziac acid (**11**) only as HC compound, would have been possibly described in the past as a chemically distinct species. However, these specimens, recognized as chemotype **iv,** appear strictly related with those of chemotype **v**, containing salazinic (**5**) and norstictic (**13**) acids as HC compounds, as some chemically intermediate specimens (chemotype **vi**) were detected.
Since there are not morphological or distributional differences, non-isidiate morphotypes producing both salazinic (**5**) and norstictic (**13**) acids and/or menegazziaic acid (**11**), and the respective LC and trace compounds (chemotypes **iv**-**vi**), may be thus also considered as new chemical varieties representative of the species group including *X. sublaevis*-*X. protomatrae*-*X. cumberlandia*, according to the approach recently adopted for Hungarian collections of *X. pulvinaris* (GYELN.) AHTI & D. HAWKSW. and *X. subdiffluens* HALE containing unforeseen norstictic acid (**13**) [37]. Similarly, on the basis of their phenotype, isidiate thalli with both salazinic acid (**5**) and stictic (**10**) -constictic (**2**) -cryptostictic (**9**) acids (chemotypes **i**-**ii**) could be considered a new chemical variety of *X. conspersa*.

Genotypic variability

The 48 *Xanthoparmelia* specimens represented 16 ITS haplotypes, generally ascribable to three (ITS/A, ITS/B-F and ITS/G-P) divergent haplotype groups (*Fig. 2*). To accomplish research objective **II**, we considered genotypic variability in terms of (a) distance values between and within the ITS haplotype groups, (b) connection between morpho-chemical phenotypes and ITS haplotypes, and (c) phylogenetic placement of the obtained ITS sequences with respect to those available in NCBI for usnic-acid (**18**) containing *Xanthoparmelia*.

(a) A threshold between intraspecific and interspecific genetic distances in Parmeliaceae, expressed in terms of nucleotide substitution per site (s/s) in ITS sequences, was indicated at 0.015 s/s [34]. However, in *Xanthoparmelia*, distances >0.16 were generally found between species previously included in separate genera, while species delimited by chemical characteristics and subtle morphological traits mostly showed strongly lower distance values (<0.015 s/s) [17][34].
Distance between haplotypes ITS/A and ITS/B-F was approx. 0.18 s/s, strongly higher than the threshold between intraspecific and interspecific distances. A lower distance of approx. 0.075 separated the isidiate specimens of the haplotype group ITS/B-F and the non-isidiate haplotypes ITS/G-P, which showed a maximum internal genetic distance of 0.032 and 0.016 respectively. Accordingly, in terms of genetic distances, different haplotype groups should be likely related to different species, but more than one species may even lie within each of the haplotype groups ITS/B-F and ITS/G-P.

(b) The annotated haplotype network of the ITS region exemplifies the correlation between the chemical and genotypic variability of the 48 specimens (*Fig. 2*). The distinct haplotype groups ITS/A and ITS/B-F were related to the isidiate morphotypes on outcrop 2, sharing the production of constictic (**2**), cryptostictic (**9**), stictic (**10**), norstictic (**13**) acids, with their associated LC compound peristictic (**6**) and from trace (chemical group **i**) to high (chemical group **ii**) amounts of salazinic acid (**5**). The haplotype group ITS/G-P was represented on both the outcrops and included all the non-isidiate specimens (chemical groups **iv-vi**), secreting salazinic acid (**5**) and/or menegazziaic acid (**11**), with their associated LC compounds, and the only isidiate specimen producing stictic acid (**10**) and related compounds, but also menegazziaic acid (**11**) (chemical group **iii**). No correspondence between the different ITS/G-P haplotypes and the variability in the relative abundance of salazinic acid (**5**) and menegazziaic acid (**11**), or with the different non-isidiate morphotypes was detected (*Table S2* in the Supporting information). This finding, combined with the detection of a common chemical profile in the

distinct haplotype groups ITS/A and ITS/B-F, confirms the limited value of medullary chemistry in delimiting natural groups in *Xanthoparmelia* [17][18][30].

(c) In a phylogenetic analysis based on the ITS sequences, aligned with those available in NCBI, the specimens of haplotype groups ITS/A and ITS/B-F clustered separately in two well supported clades (*Fig. 3*). The cluster including the haplotype group ITS/A, containing one specimen each for chemotypes **i** and **ii**, exclusively included sequences of the isidiate species *X. tinctina*, which was previously recognized to be phylogenetically well separated from most of other European green-yellow Xanthoparmelias [31]. The haplotypes ITS/C-F, similarly representative of both the chemotypes **i** and **ii**, clustered with sequences of European specimens of the isidiate *X. conspersa* and *X. isidiovagans* O. Blanco, A. Crespo, Divakar & Elix, but also with the non-isidiate *X. vicentei* A. Crespo, M.C. Molina & Elix. The haplotype ITS/B was included in a paraphyletic cluster, which also included other isidiate and non-isidiate species from Europe and North-America.

The specimens of the haplotype group ITS/G-P (with the exception of haplotype ITS/O) clustered in a third clade, including different lineages which did not reveal any correspondence with the detected chemical patterns, *i.e.* with the relative abundance of salazinic (**5**) and/or menegazziaic (**11**) acids, or with the specimen provenience from the two outcrops. The cluster included sequences of European and American specimens of non-isidiate species, including *X. protomatrae* and *X. stenophylla*, without revealing any correspondence between the different haplotypes and the different morphological and chemical characters of the species (*Fig. 3*).

On the whole, as previously reported at the regional and continental scale [17][18][30], the combination of morpho-chemical and phylogenetic analyses on *Xanthoparmelia* specimen sets sampled at the local scale of two rock outcrops highlighted variability patterns only partially compatible with the traditional species circumscription. The discussion of the taxonomic placement of the surveyed specimens at the light of phylogenetic analyses is beyond the content of this paper, as the focus should be moved to a wider geographic scale, and the analyses of more genes should be necessary (see [17][18]). Nevertheless, it is worth noting that ITS barcoding, widely used in species- and population-level studies on lichenized ascomycetes [17][21], may not guarantee the discrimination of chemically homogeneous or dishomogeneous lineages of *Xanthoparmelia*.

As only clearly demarcated thalline "rosettes" were collected for this study, the fact that sequences from the specimens of the related chemotypes **i**-**ii** variously clustered with *X. tinctina* and the isidiate species of the *Xanthoparmelia* "core" group, including *X. conspersa*, suggests that the examined isidiate thalli may contain multiple mycobionts of *X. tinctina* and *X. conspersa*. Accordingly, intrathalline metabolic and physiological differences were recognized in "*Parmelia conspersa*" and putatively explained by the presence of a different mycobiont in each lobe or in different parts of thallus [46]. The hypothesized mycobiont co-occurrence may also explain the unreported detection of salazinic acid (**5**) and stictic (**10**) -constictic (**2**) -cryptostictic (**9**) acids in the same isidiate thalli, and may suggest some analogies with the recently described LSMs acquisition by the crustose lichen *Ophioparma ventosa* (L.) Norman from overgrown thalli of different species [47]. Nevertheless, our ITS sequences were obtained for each thallus upon DNA extractions from multiple lobe fragments and the sequences did not reveal mixed spectrograms, and only isidia morphologically suitable for *X. conspersa* were observed on all the specimens.

Similarly, thalli of chemotype **vi**, intermediate between **iv** and **v**, may be explained by the presence in different lobes of mycobionts producing menegazziaic (**11**) and salazinic (**5**) acids, respectively. However, both these metabolites are produced in thalli phylogenetically and morphologically related, and the different production may be possibly related to micro-environmental factors, which have been hypothesized to drive the morphological and chemical variability [48][49], but with poor experimental support [50][51]. With this regard, in the non-isidiate morphotypes, we found a positive correlation of salazinic acid (**5**) and related compounds with mineral macronutrients in thalli, and negative with mineral micronutrients derived from the bedrock, as quantified by XRF (*Tables S4A-C* in the Supporting Information), while menegazziaic acid (**11**), and related metabolites, showed an opposite trend. The observed tendency may agree with a different role of the different LSMs in the metal homeostasis of thalli [13][52][53], but further experimental support is needed to consider other micro-environmental variables and to analyze elemental effects on the LSM synthesis by *Xanthoparmelia* in controlled conditions.

Conclusions

Our work showed that a high level of morpho-chemical variability in *Xanthoparmelia* can be also detected at the very local scale of rock outcrops, not only between, but also within different phylogenetic lineages. We confirmed the co-occurrence of different *Xanthoparmelia taxa* [39][40], primarily distinguishable from morphological characters, as the presence/absence of isidia (morphotypes M-I/M-VI vs. M-VII/M-IX), and partially supported by ITS barcoding (haplotype groups ITS/A, ITS/B-F, ITS/G-P). However, we also found that (**I**) certain morphotypes can be chemically variable in terms of presence/absence and concentrations of LSMs, and that some morpho-chemical phenotypes fit with difficulty into the available species descriptions. Accordingly, morphological features may poorly address the collection of chemically homogeneous thalli to test and exploit LSMs. Moreover, (**II**) although a part of (morpho)-chemical variability was related to divergent haplotype groups of the ITS barcode, strong chemical differences also characterized each haplotype group and, even, the same haplotype. Accordingly, the fungal barcode appears unsuitable for predicting the chemical variability of *Xanthoparmelia* thalli, even on a single rock outcrop.

In conclusion, collections of *Xanthoparmelia* thalli performed at a very local level may not guarantee the availability of chemically homogeneous materials [see 22]. As the chemical variability also concerns the occurrence and content of LSMs known as bioactive compounds, this finding has to be taken into particular account when tests and exploitation of *Xanthoparmelia* crude extracts are planned, also considering LC and trace compounds [see 6-7]. With this regard, our results suggest that a careful sampling approach combined with mass spectrometry techniques should be necessarily considered as an effective method for the characterization of chemical variability in lichens from local to higher spatial scales.

Finally, whatever the nature of the unidentified compounds **12**, **15** and **16**, this study also indicated that a single *Xanthoparmelia* community may be a source of several LSMs still unlisted in available catalogues [44][45]. While only the alpine habitat has been suggested as untapped source of bioactive lichen metabolites [3], other biomes of the Alps at lower altitudes, rich of Xanthoparmelias, may harbour some unknown diversity in LSMs.

Experimental Section

Lichen material

Two rock outcrops (ca. 50×50 m) 60 km apart in Western Italian Alps (site 1: UTM ED50, N 4998464, E 354063, Borgata Tignai, Bussoleno, Susa Valley; site 2: UTM ED50, N 5068915, E 370323, Borgata Croux, Saint-Christophe, Aosta Valley), largely colonized by *Xanthoparmelia* thalli, were selected to examine their morphological, chemical and genotypic variability. The two outcrops have similar elevation (600 and 800 m a.s.l., respectively), xeric microclimate and gneiss lithology (*Fig. S3* in the Supporting Information). PVGIS estimates [54] indicated similar average sums of global irradiation per square meter (H_m = 1200 kWh m^{-2} and 1300 kWh m^{-2} for sites 1 and 2, respectively, at inclination = 0° and orientation = 0°). Average annual air temperature and precipitation, monitored in close urban areas, were also similar (9.7°C and 799 mm in Susa; 11.4°C, respectively, and 805 mm in Aosta; it.climate-data.org).

At each outcrop, 7 independent 50×50 cm plots were established on surfaces sharing similar (micro-)environmental features (direct solar irradiation, regular micromorphology, absence of cracks, slope <30°). Each plot was surveyed using a square grid divided into 25 quadrats (10×10 cm). Total *Xanthoparmelia* cover within each plot was estimated visually. The frequency of different morphotypes within each plot (as the sum of their occurrences within the grid quadrats) was evaluated with reference to traits traditionally used to define the species boundaries (including thallus adnation, lobation, lower surface colour and occurrence of isidia as reproductive structures [23]).

In October 2012, we collected from each outcrop twenty-four adult thalli (diameter greater than 4 cm), which were definitely recognizable as distinct foliose rosettes (*i.e.* collection of thalli coalescing into larger patches or scattered lobes was avoided). The number of thalli collected for each morphotype (M-I/M-IX) was approx. proportional to their abundance in the surveyed plots. Collections were made on fully sun-exposed horizontal rock-surfaces, on public lands where sampling permits were not required. All specimens have been deposited at the *Herbarium Universitatis Taurinensis* (TO), Italy (vouchers TO3662-TO3663 as *Xanthoparmelia* cf. *tinctina* (Maheu & A. Gillet) Hale; vouchers TO3651-TO3653, TO3657, TO3659-TO3660, TO3665, TO3671-TO3672 as *X.* cf. *conspersa* (Ach.) Hale; other vouchers TO3654-TO3656, TO3658, TO3661, TO3664, TO3666-TO3670, TO3673-TO3699 as *X.* cf. *stenophylla* (Ach.) Ahti & D.Hawksw.).

Identification and quantification of LSMs by HPLC-DAD-ESI-MS_2 and UPLC-HDR-DAD

LSMs were extracted from a pool of at least three different marginal lobes of each thallus (ca. 25 mg). The lobes were grinded and incubated in acetone (VWR, Italy) at a solid:liquid ratio of 1:50 (w/v) for 10 h at room temperature in the dark. Three sonication steps of 15 min were performed, at room temperature, at the beginning and at the end of the incubation. Acetone extracts were then filtered at 0.45 µm and dried using a Centrifugal Vacuum Concentrator combined with the CentriVap Cold Trap (Labconco, USA). The residues were redissolved in acetone and stored at -20°C until use. Atranorin (40 µg ml^{-1}) (Sigma-Aldrich, USA) was used as internal standard for the quantification of detected compounds (*Chemical formulae 1*).

Compound identification was performed by HPLC-DAD-ESI-MS_2 using a 1200 HPLC (Agilent Technologies, USA) equipped with a Luna C18 reversed-phase column (3.00 µm, 150 x 3.0 mm I.D., Phenomenex, USA). The binary solvent system was: A) acidified double distilled water (Millipore, USA) with 0.1% v/v formic acid (Sigma-Aldrich, USA) and B), acetonitrile (Carlo-Erba, Italy) with 0.1% v/v formic acid. Chromatography was carried out at a flow rate of 0.2 ml min^{-1}, column temperature was maintained at 25°C and the following solvent gradient was used: 40% of B for 1 min, 55% B at 4.5 min, 62% B at 5 min, 65% B at 14 min, 98% B at 16 min and 40% B at 18 min. The initial mobile phase was re-established for 8 min before the next injection. Mass spectrometry analyses were performed in negative mode with a 6330 Series Ion Trap (Agilent Technologies, USA) equipped with an electrospray ionization source (ESI). The capillary voltage was set at -1800 V and drying gas flowed at 10 L min^{-1} and 325 °C. The recorded scan range was 50-700 *m/z*. The absorbance signals were recorded at 290.0, 325.0, 239.0, 317.0 and 252.0 nm according to reported UV-Vis spectra of *Xanthoparmelia* LSMs [45].

Quantitative analyses were performed with a 1290 UPLC (Agilent Technologies, USA) equipped with a reversed-phase column ZORBAX Eclipse C18 (50 mm × 2.1 mm, 1.8 µm). The mobile phase was composed of 0.1% trifluoroacetic acid in double distilled water (A) and 0.1% trifluoroacetic acid in acetonitrile (B). Chromatography was performed at 0.5 ml min^{-1} with the following solvent gradient: at 0 min 10% of B, at 1 min 15% B, at 1.2 min 40% B , at 8 min B was increased to 70%, at 8.3 min B was used for 1.5 min at 98 % to wash the column, finally at 9.9 min the concentration of B solvent was re-established to 10%. The column was re-conditioned before a new analysis. Injection volume was 0.3 µl. The system was equipped with two Agilent 1290 Infinity Detectors (Agilent Technologies, Germany) operating in HDR mode at 40 Hz with a 60 mm and a 3.7 mm path length cells, respectively. The

Agilent HDR-DAD operative mode based on the use of two diode array detectors that were equipped with flow cells at different path lengths. The combination absorbance signals from both DAD detectors significantly increases the quantitative linear range. The absorbance signals were recorded at 290.0, 325.0, 239.0, 317.0 and 252.0 nm according to reported spectra of identified compounds [45]. Quantitative data were reported as equivalent units of atranorin (μg g^{-1} dry wt) by comparison with the internal standard. The relative amounts can only be properly compared within the same compound because known or potential compoud-specific differences in UV absorption limit the comparability of signals between substances [52]. Nevertheless, the range of variation of UV extinction coefficients available [45] for compounds **3**, **5**, **9**, **10**, **13**, **14**, **17** and **18** suggests the reliability of a comparison between LSMs based on wide concentration categories: highly-concentrated (>600 μg g^{-1} dry wt; HC), low-concentrated (25< μg g^{-1} dry wt <600; LC) and trace (<25 μg g^{-1} dry wt) amounts.

DNA extraction, amplification, sequencing and phylogenetic analyses

DNA was extracted from the 48 specimens using the DNeasy Plant MiniKit (Qiagen, USA). PCR amplifications were performed using DreamTaq DNA polymerase (Fermentas, USA) in a Whatman Biometra T-Gradient Thermalcycler (Whatman Biometra, Germany). The ITS1-5.8S-ITS2 region of rDNA (primers ITS1F-ITS4 [55]), widely analyzed in species- and population-level studies on lichenized ascomycetes, including *Xanthoparmelia* [17], were amplified by PCR and sequenced by Beckman Coulter Genomics (Hope End, UK). All sequences generated in this study are available in GenBank under the Accession Ns. KP129443-KP129487.

Statistical analyses

LSM quantitative data matrix obtained by UPLC analyses was processed with a Principal Coordinate Analysis (PCoA: symmetric scaling, centring samples by samples, centring species by species) [56]. A classification of the specimens with reference to their chemical contents was also performed (UPGMA, Normalized Camberra as coefficient). Ordination and classification analyses were performed using the softwares CANOCO 4.5 [56] and SYN-TAX 2000 [57], respectively.

ITS sequences were curated in Mega 4 [58], aligned with MUSCLE [59] and used as queries in BLAST searches [60]. Haplotype and nucleotide diversity was calculated in Mega 4 [58]. The gene genealogies between sequences were determined by statistical parsimony using TCS1.21 software [61]. Prior to phylogenetic analysis, jModelTest v. 2.1.7 [62] was employed to estimate the best-fit model of nucleotide substitution for the dataset. Phylogenetic analyses were performed using MrBayes v. 3.2.2 [63]. The partitioned Bayesian analysis was performed with Tim2ef+G, K80 and TrNef+G nucleotide substitution models for ITS1, 5.8S rRNA gene and ITS2 regions, respectively. The Markov chain Monte Carlo was run for 10 million generations. The phylogenetic tree shows the nodes that are supported by at least ≥ 0.70 posterior probability: nodes with lower support were collapsed.

Supplementary Material

Supporting information for this article is available on the WWW under http://dx.doi.org/10.1002/MS-number.

Table S1. Phenotypic delimitation of *Xanthoparmelia* species with yellow-green thalli, because of usnic acid (**18**) in the upper cortex, reported for Europe.

Table S2. Lichen secondary metabolites detected and quantified in the yellow-green *Xanthoparmelia* specimens by HPLC-DAD-ESI-MS_2 and UPLC-HDR-DAD, respectively. (A) Concentration distribution throughout the specimen set and (B) individual concentrations.

Table S3. Phenotypic characters of non-European, usnic acid (**18**)-containing *Xanthoparmelia* species considered in the Results and Discussion section.

Tables S4. (A) XRF elemental contents analyses of the yellow-green *Xanthoparmelia* (haplotype group ITS/G-P // Chemotypes iii-vi). Contents (% av. ± s.e.) for the specimen set (SS; n=38) and the individuals; (B) Pearson's correlation coefficients between element contents; (C) Pearson's correlation coefficients between medullary elemental contents and secondary metabolites (list in *Table 1*) in *Xanthoparmelia* (haplotype group ITS/G-P // Chemotypes iii-vi).

Fig. S1. HPLC-DAD-ESI-MS_2 spectra of unidentified metabolites from *Xanthoparmelia*.

Fig. S2. Cluster analysis of the specimen set based on the quantitative analyses by UPLC-HDR-DAD.

Fig. S3. Study sites.

Acknowledgements

EM was the recipient of a postdoctoral fellowship (RICERCA FSE 2011-2012, funded by the European Union, Italian Ministry of Labour and Social Policies, Regione Autonoma Valle d'Aosta: agreement 10016/DPLF/28June2012). The authors are grateful to three anonymous reviewers for helpful and constructive comments, to F. Rolfo (University of Torino) for accession to XRF spectroscopy, to A. Desirò (University of Torino) and C. Murat (INRA, Nancy,

France) for helpful discussions on DNA analyses, and to M. Barbieri (Agilent Technologies) for the kind use of the Agilent 1290 UPLC-HDR-DAD. This work was partly supported by Biosfered S.r.l.

Author Contribution Statement

Conceived and designed the experiments: EM RP MEM SEFL. Performed the experiments: EM AO SEFL. Analyzed the data: SEFL AO EM. Contributed reagents/materials/analysis tools: RP MEM. Wrote the paper: SEFL EM AO MEM.

References

[1] J. A. Elix, E. Stocker-Wörgötter, in 'Lichen Biology (Second Edition)', Ed. T. H. Nash III, Cambridge University Press, Cambridge, 2008, p. 104.

[2] K. Molnár, E. Farkas, 'Current results on biological activities of lichen secondary metabolites: a review', *Zeitschrift für Naturforschung C*, **2010**, *65*, 157-173.

[3] J. Boustie, S. Tomasi, M. Grube, 'Bioactive lichen metabolites: alpine habitats as an untapped source', *Phytochem. Rev.*, **2011**, *10*, 287-307.

[4] G. Shrestha, L. L. St. Clair, 'Lichens: a promising source of antibiotic and anticancer drugs', *Phytochem. Rev.*, **2013**, *12*, 229-244.

[5] B. Ranković, M. Kosanić, in 'Lichen Secondary Metabolites', Ed. B. Ranković, Springer International Publishing Switzerland, Cham (CH), 2015, p. 1.

[6] X. Yu, Q. Guo, G. Su, A. Yang, Z. Hu, C. Qu, Z. Wan, R. Li, P. Tu, X. Chai, 'Usnic acid derivatives with cytotoxic and antifungal activities from the lichen *Usnea longissima*', *J. Nat. Prod.* **2016**, *79*, 1373-1380.

[7] P. Le Pogam, A.-C. Le Lamer, B. Siva, B. Legouin, A. Bondon, J. Graton, D. Jacqemin, I. Rouaud, S. Ferron, W. Obermayer, K. S. Babu, J. Boustie, 'Minor pyranonaphthoquinones from the apothecia of the lichen *Ophioparma ventosa*', *J. Nat. Prod.*, **2016**, *79*, 1005-1011.

[8] D. L. Hawksworth, in 'Lichenology: progress and problems', Eds. D. H. Brown, D. L. Hawksworth, R. H. Bailey, Academic Press, London, 1976, p. 139.

[9] G. Holzmann, C. Leuckert, 'Applications of negative fast atom bombardment and MS/MS to screening of lichen compounds', *Phytochemistry*, **1990**, *29*, 2277-2283.

[10] G. B. Feige, H. T. Lumbsch, S. Huneck, J. A. Elix, 'Identification of lichen substances by a standardized high-performance liquid chromatographic method', *J. Chromatogr. A*, **1993**, *646*, 417-427.

[11] P. Le Pogam, B. Legouin, A.-C. Le Lamer, J. Boustie, D. Rondeau, 'Analysis of the cyanolichen *Lichina pygmaea* metabolites using *in situ* DART-MS: from detection to thermochemistry of mycosporine serinol', *J. Mass Spectrom.*, **2015**, *50*, 454-462.

[12] P. Le Pogam, A. Schinkovitz, B. Legouin, B., A.-C. Le Lamer, J. Boustie, P. Richomme, 'Matrix-free UV-laser desorption ionization mass spectrometry as a versatile approach for accelerating dereplication studies on lichens', *Anal. Chem.*, **2015**, *87*, 10421-10428.

[13] M. Hauck, J. Böning, M. Jacob, S. Dittrich, I. Feussner, C. Leuschner, 'Lichen substance concentrations in the lichen *Hypogymnia physodes* are correlated with heavy metal concentrations in the substratum', *Env. Exp. Bot.*, **2013**, *85*, 58-63.

[14] D. Parrot, S. Jan, N. Baert, S. Guyot, S. Tomasi, 'Comparative metabolite profiling and chemical study of *Ramalina siliquosa* complex using LC-ESI-MS/MS approach', *Phytochemistry*, **2013**, *89*, 114-124.

[15] D. Parrot, T. Peresse, E. Hitti, D. Carrie, M. Grube, S. Tomasi, 'Qualitative and spatial metabolite profiling of lichens by a LC–MS approach combined with optimised extraction', *Phytochem. Anal.*, **2015**, *26*, 23-33.

[16] K. Molnár, K., E. Farkas, 'Depsides and depsidones in populations of the lichen *Hypogymnia physodes* and its genetic diversity', *Ann. Bot. Fenn.*, **2011**, *48*, 473-482.

[17] S. D. Leavitt, L. Johnson, L. L. St. Clair, 'Species delimitation and evolution in morphologically and chemically diverse communities of the lichen-forming genus *Xanthoparmelia* (Parmeliaceae, Ascomycota) in western North America', *Am. J. Bot.*, **2011**, *98*, 175-188.

[18] S. D. Leavitt, L. A., Johnson, T. Goward, L. L. St. Clair, 'Species delimitation in taxonomically difficult lichen-forming fungi: an example from morphologically and chemically diverse *Xanthoparmelia* (Parmeliaceae) in North America', *Mol. Phylogenet. Evol.* **2011**, *60*, 317-332.

[19] G. Shrestha, A. M. El-Naggar, L L. St Clair, K. L. O'Neill, 'Anticancer activities of selected species of North American lichen extracts', *Phytotherapy Res.*, **2015**, *29*, 100-107.

[20] P. Shukla, D. K. Upreti, L. M. Tewari, 'Secondary metabolite variability in lichen genus *Usnea* in India: A potential source for bioprospection', *G-Journal of Environmental Science and Technology*, **2015**, *2*, 44-55.

[21] C. G. Boluda, V. J. Rico, A. Crespo, P. K. Divakar, D. L. Hawksworth, 'Molecular sequence data from populations of *Bryoria fuscescens* s. lat. in the mountains of central Spain indicates a mismatch between haplotypes and chemotypes', *Lichenologist*, **2015**, *47*, 279-286.

[22] P. Le Pogam, G. Herbette, J. Boustie, in 'Recent Advances in Lichenology - Vol. 1: Modern methods and approaches in biomonitoring and bioprospection', Eds. D. K. Upreti, P. K. Divakar, V. Shukla, R. Bajpal, Springer, New Delhi, 2015, p. 229.

[23] M. E. Hale, 'A synopsis of the lichen genus *Xanthoparmelia* (Vainio) Hale (Ascomycotina, Parmeliaceae)', *Smithson. Contrib. Bot.*, **1990**, *74*, 1-250.

[24] G. Amo de Paz, M. P. Gómez-Serranillos, O. M. Palomino, E. González-Burgos, M. E. Carretero, A. Crespo, 'HPLC isolation of antioxidant constituents from *Xanthoparmelia* ssp.' *J. Pharm. Biomed. Anal.*, **2010**, *53*, 165-171.

[25] G. Laska, S. Kiercul, M. Stocki, A. Bajguz, D. Pasco, 'Cancer-chemopreventive actvity of secondary metabolites isolated from *Xanthoparmelia conspersa* lichen', *Planta Medica*, **2015**, *81*, PM_59.

[26] M. McEvoy, L. Nybakken, K. A. Solhaug, Y. Gauslaa, 'UV triggers the synthesis of the widely distributed secondary lichen compound usnic acid', *Mycological Progress*, **2006**, *5*, 221-229.

[27] C. Deduke, M. D. Piercey-Normore, 'A potential trade-off with stictic acid improves ascospore viability in *Xanthoparmelia cumberlandia*', *Bryologist*, **2014**, *117*, 290-296.

[28] R. Dailey, S. Roger, M. Raisbeck, C. Jesse, 'Analysis of salazinic, norstictic, and usnic acid in *Xanthoparmelia chlorochroa* by Ultra-Performance Liquid Chromatography/Tandem Mass Spectrometry', *J. AOAC Int.*, **2010**, *93*, 1137-1142.

[29] J.A. Elix, 'Progress in the generic delimitation of *Parmelia* sensu lato lichens (Ascomycotina: Parmeliaceae) and a synoptic key to the Parmeliaceae', *Bryologist*, **1993**, *96*, 359-383.

[30] U. Jayalal, P. K. Divakar, S. Joshi, S. Ok Oh, J. A. Kim, J.-S. Hur, 'Overview of *Xanthoparmelia* taxa from South Korea including the description of two new species (Parmeliaceae, Ascomycota)', *Phytotaxa*, **2014**, *181*, 96-109.

[31] O. Blanco, A. Crespo, J. A. Elix, D. L. Hawksworth, H. T. Lumbsch, 'A molecular phylogeny and a new classification of parmelioid lichens containing *Xanthoparmelia*-type lichenan (Ascomycota: Lecanorales)', *Taxon*, **2004**, *53*, 959-975.

[32] B. P. Hodkinson, J. C. Lendemer, 'Molecular analyses reveal semi-cryptic species in *Xanthoparmelia tasmanica*', *Bibliotheca Lichenologica*, **2011**, *106*, 108-119.

[33] C. L. Schoch, K. A. Seifert, S. Huhndorf, V. Robert, J. L. Spouge, C. A. Levesque, W. Chen, Fungal Barcoding Consortium, 'Nuclear ribosomal internal transcribed spacer (ITS) region as a universal DNA barcode marker for Fungi', *PNAS*, **2012**, *109*, 6241-6246.

[34] R. Del-Prado, P. Cubas, H. T. Lumbsch, P. K. Divakar, O. Blanco, G. Amo de Paz, M. C. Molina, A. Crespo, 'Genetic distances within and among species in monophyletic lineages of Parmeliaceae (Ascomycota) as a tool for taxon delimitation', *Mol. Phylogenet. Evol.*, **2010**, *56*, 125-133.

[35] D. L. Hawksworth, O. Blanco, P. K. Divakar, T. Ahti, A. Crespo, 'A first checklist of parmelioid and similar lichens in Europe and some adjacent territories, adopting revised generic circumscriptions and with indications of species distributions', *Lichenologist*, **2008**, *40*, 1-21.

[36] P. Kanigowski, A. Flakus, M. Oset, A. Kowalewska, M. Rykaczewki, M. Kukwa, 'The lichen family Parmeliaceae in Poland. *Xanthoparmelia* species containing usnic acid', *Herzogia*, **2016**, *29*, 108-119.

[37] E. Farkas, L. Kursinszki, É. Szoke, K. Molnár, 'New chemotypes of the lichens *Xanthoparmelia pulvinaris* and *X. subdiffluens* (Parmeliaceae, Ascomycota)', *Herzogia*, **2015**, *28*, 679-689.

[38] S. D. Leavitt, C. S. Moreau, H. T. Lumbsch, in 'Recent Advances in Lichenology - Vol. 2: Modern methods and approaches in lichen systematics and culture techniques', Eds. D. K. Upreti, P. K. Divakar, V. Shukla, R. Bajpal, Springer, New Delhi, 2015, p. 11.

[39] S. D. Leavitt, L. L. St. Clair, 'Lichens of the Boulder Mountain Plateau, Wayne County, Utah, USA', *Evansia*, **2008**, *25*, 85-89.

[40] G. Rizzi, P. Giordani, 'The ecology of the lichen genus *Xanthoparmelia* in Italy: an investigation through spatial scales', *Plant Biosystems*, **2013**, *147*, 33-39.

[41] V. J. Poelt, 'Die taxonomische Behandlung von Artenpaaren bei den Flechten', *Bot. Notiser*, **1972**, *125*, 76-81.

[42] P. Giordani, P. Nicora, I. Rellini, G. Brunialti, J. A. Elix, 'The lichen genus *Xanthoparmelia* (Ascomycotina, Parmeliaceae) in Italy', *Lichenologist*, **2002**. *34*, 189-198.

[43] P. L. Nimis, 'The lichens of Italy. A second annotated catalogue', Edizioni Università di Trieste, Trieste, 2016.

[44] J. A. Elix, 'A catalogue of standardized chromatographic data and biosynthetic relationships for lichen substances. Third Edition', published by the author, Canberra, 2014. (Available at: www.anbg.gov.au/abrs/lichenlist/Chem%20Cat%203.pdf; accessed on 29th June 2016).

[45] S. Huneck, I. Yoshimura, 'Identification of lichen substances', Springer, Berlin, 1996.

[46] D. Fahselt, in 'Lichen biology', Ed. T. H. Nash III, Cambridge University Press, Cambridge, 1996, p. 181.

[47] P. Le Pogam, B. Legouin, A. Geairon, H. Rogniaux, F. Lohézic-Le Dévéhat, W. Obermayer, J. Boustie, A.-C. Le Lamer, 'Spatial mapping of lichen specialized metabolites using LDI-MSI: Chemical ecology issues for *Ophioparma ventosa*' Scientific Reports, **2016**, *6*, 37807.

[48] C. Hametner, E. Stocker-Wörgötter, in 'Recent Advances in Lichenology - Vol. 2: Modern methods and approaches in lichen systematics and culture techniques', Eds. D. K. Upreti, P. K. Divakar, V. Shukla, R. Bajpal, Springer, New Delhi, 2015, p. 95.

[49] Y. Joshi, M. Tripathi, P. K. Divakar, D. K. Upreti, 'A note on the occurrence of *Xanthoparmelia saxeti* (Stizenb.) Amo, A. Crespo, Elix & Lumbsch in India', *Webbia*, **2014**, *69*, 137-139.

[50] C. Deduke, B. Timsina, M. R. Piercey-Normore, in 'International perspectives on global environmental change', Ed. S. Young, InTech, Croatia, 2012, p. 197.

[51] T. H. Nash III, M. Zavada, 'Population studies among Sonoran Desert species of *Parmelia* subg. *Xanthoparmelia* (Parmeliaceae)', *Am. J. Bot.*, **1977**, *64*, 664-669.

[52] M. Hauck, S. Huneck, J. A. Elix, A. Paul, 'Does secondary chemistry enable lichens to grow on iron-rich substrates?', *Flora*, **2007**, *202*, 471-478.

[53] S. E. Favero-Longo, in 'Plant ecology and evolution in harsh environments', Ed. N. Rajakaruna, T. Harris, R. Boyd, Nova Publishers, New York, 2014; p. 53.

[54] PVGIS © European Communities; 2001–2012. (Available at: re.jrc.ec.europa.eu/pvgis/about_pvgis/about_pvgis.htm; accessed on 29th June 2016).

[55] M. Gardes, T. D. Bruns, 'ITS primers with enhanced specificity for basidiomycetes – Application to the identification of mycorrhizae and rusts', *Mol. Ecol.*, **1993**, *2*, 113-118.

[56] C. J. F. Ter Braak, P. Šmilauer, 'CANOCO reference manual and Canodraw for Windows user's guide: software for canonical community ordination (version 4.5)' Microcomputer Power, Ithaca (NY), 2002.

[57] J. Podani, 'SYN-TAX 2000. Computer programs for data analysis in ecology and systematics. User's manual', Scientia, Budapest, 2001.

[58] K. Tamura, J. Dudley, M. Nei, S. Kumar, 'MEGA: Molecular Evolutionary Genetics Analysis (MEGA) software version 4.0.', *Mol. Biol. Evol.*, **2007**, *24*, 1596-1599.

[59] R. C. Edgar, 'MUSCLE: a multiple sequence alignment method with reduced time and space complexity', *BMC Bioinf.*, **2004**, 5, 113.

[60] S. F. Altschul, T. L. Madden, A. A. Schäffer, J. Zhang, Z. Zhang, W. Miller, D. J. Lipman, 'Gapped BLAST and PSI-BLAST: a new generation of protein database search programs', *Nucleic Acids Res.*, **1997**, *25*, 3389-3402.

[61] M. Clement, D. C. K. A. Posada, K. A. Crandall, 'TCS: a computer program to estimate gene genealogies', *Mol. Ecol.*, **2000**, *9*, 1657-1659.

[62] D. Darriba, G. L. Taboada, R. Doallo, D. Posada, D., 'jModelTest 2: more models, new heuristics and parallel computing', *Nature Methods*, **2012**, *9*, 772.

[63] F. Ronquist, M. Teslenko, P. van der Mark, D. L. Ayres, A. Darling, S. Höhna, B. Larget, L. Liu, M. A. Suchard, J. P. Huelsenbeck, J.P., 'MrBayes 3.2: efficient Bayesian phylogenetic inference and model choice across a large model space', *Syst. Biol.*, **2012**, *61*, 539-542.

Table 1. Morphotypes of usnic acid (**18**)-containing *Xanthoparmelia* recognized on outcrops 1 and 2 on the basis of: isidia occurrence and shape (ISI: 0, isidia absent; 1, presence of isidia from (sub-)globose to cylindrical and branched), lower surface colour of thalli (COL: 0, black; 1, dark brown; 2, pale to dark-brown or mottled; 3, pale brown), thallus adnation (ADN: 1, loosely adnate; 2, loosely adnate to adnate; 3, adnate to tightly adnate) and lobe shape (LOB: 0, subirregular, or subirregular to sublinear; 1, sublinear to laciniate). Definitions and reference figures for these traits in [23]. None of the morphotypes showed a maculate upper-surface of lobes (*i.e.* another morphological feature having taxonomic significance in the traditional recognition of *Xanthoparmelia* species).

Morphotype	ISI	COL	ADN	LOB	Outcrop	Frequency (%, on outcrop 1,2)	Examined specimens (n, from outcrops 1, 2)	Symbols (outcrops 1, 2)
M-I	0	1	2	0	1	1, 0	2, 0	+, -
M-II	0	2	1	0	1, 2	43, 14	8, 3	○, ●
M-III	0	2	1	1	1	3, 0	2, 0	×, -
M-IV	0	2	2	0	1, 2	29, 18	4, 4	□, ■
M-V	0	2	3	0	1, 2	15, 11	4, 3	◊, ♦
M-VI	0	3	1	0	1, 2	10, 25	4, 6	✧, ✦
M-VII	1	0	2	0	2	0, 14	0, 3	-, ▲
M-VIII	1	0	3	0	2	0, 16	0, 4	-, ▼
M-IX	1	1	2	0	2	0, 2	0, 1	-, ▶

Table 2. Lichen secondary metabolites of the examined yellow-green thalli of *Xanthoparmelia*. Molecular ions ([M-H]$^-$), product ions (relative abundance), frequency, concentration range (µg g^{-1} dry wt) and distribution [% presence as highly-concentrated (HC), low-concentrated (LC) or trace content]. Most abundant compounds (max > of 600 µg g^{-1} dry wt) are shown in bold.

	Compounds	[M-H]$^-$(m/z)	Product ions (m/z)				Frequency (n/48 specimens)	Concentration range as atranorin equivalents (µg g^{-1} dry wt)		Concentration distribution (specimen %)			
								Min	Max	≤25 µg g^{-1} (trace)	25< µg g^{-1} <600 (LC)	≥600 µg g^{-1} (HC)	absent
1	Consalazinic acid	389	371 (100)	327 (43)	309 (8)		33	4	292	8.3	60.4	-	31.3
2	**Constictic acid**	401	357 (100)	313 (4.4)	283 (21)		8	806	2726	-	-	16.7	83.3
3	Protocetraric acid	373	355 (40)	329 (100)	255 (13)		29	12	68	31.3	29.2	-	39.6
4	Connorstictic acid	373	355 (100)	329 (6)	311 (48)		33	2	118	12.5	56.3	-	31.3
5	**Salazinic acid**	387	343 (100)	325 (21)	269 (8)		48	6	12054	29.2	-	70.8	-
6	Peristictic acid	401	357 (100)	313 (21)	295 (5)	269 (3)	8	36	148	2.1	14.6	-	83.3
7	Conprotocetraric acid	375	375 (63)	357 (100)	339 (6)		46	26	510	-	95.8	-	4.2
8	Substictic acid	371	353 (100)	341 (3.7)			23	2	144	14.6	33.3	-	52.1
9	**Cryptostictic acid**	387	343 (100)	299 (18)	269 (3)		9	102	2948	-	4.2	14.6	81.3
10	**Stictic acid**	385	341 (100)	297 (35)	282 (6)		9	4	4004	2.1	-	16.7	81.3
11	**Menegazziaic acid**	373	355 (66)	329 (100)	311 (94)	285 (26)	43	2	4644	54.2	2.1	33.3	10.4
12	Unknown compound	403	403 (20)	385 (100)	367 (5.7)	349 (4)	31	16	128	8.3	56.3	-	35.4
13	**Norstictic acid**	371	327 (100)	283 (14)	243 (25)	227 (29)	37	144	874	-	66.7	10.4	22.9
14	Fumarprotocetraric acid	471	355 (100)	311 (18)			12	2	12	25	-	-	75
15	Unknown compound	427	383 (15)	369 (100)	355 (4)	325 (3)	47	2	46	79.2	18.8	-	2.1
16	Unknown compound	359	344 (49)	341 (100)	326 (12)		38	2	88	54.2	25	-	20.8
17	Methylhypoprotocetraric	357	344 (51)	341 (100)	326 (11.6)		40	2	38	79.2	4.2	-	16.7
18	**Usnic acid**	343	329 (100)	299 (8.6)	259 (14)		48	1112	4010	-	-	100	-

Chemical formulae & Figure captions

Chemical formulae 1. Chemical structures of detected *Xanthoparmelia* compounds (**1-11**, **13-14**, **17-18**) and of atranorin (internal standard).

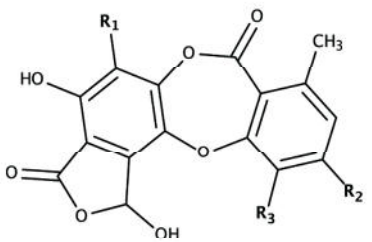

1, 2, 4, 5, 6, 8, 9, 10, 11, 13

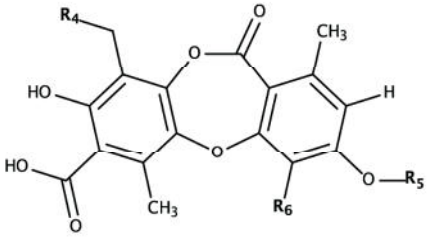

3, 7, 14, 17

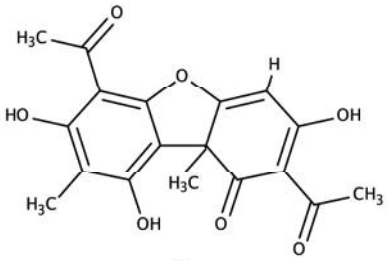

18

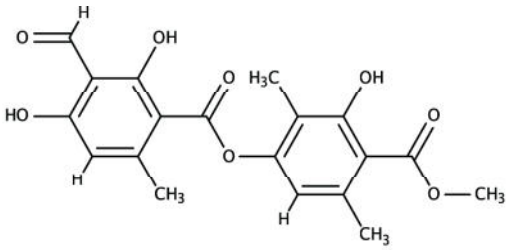

Atranorin (Internal standard)

	Compounds	R1	R2	R3	R4	R5	R6
1	Consalazinic acid	CH_2-OH	OH	CH_2-OH	-	-	-
2	Constictic acid	CH_2-OH	O-CH_3	CH-O	-	-	-
3	Protocetraric acid	-	-	-	OH	H	CH-O
4	Connorstictic acid	CH_3	OH	CH_2-OH	-	-	-
5	Salazinic acid	CH_2-OH	OH	CH-O	-	-	-
6	Peristictic acid	CH_3	O-CH_3	CO_2H	-	-	-
7	Conprotocetraric acid	-	-	-	CH_2-OH	H	CH_2-OH
8	Substictic acid	H	O-CH_3	CH-O	-	-	-
9	Cryptostictic acid	CH_3	O-CH_3	CH_2-OH	-	-	-
10	Stictic acid	CH_3	O-CH_3	CH-O	-	-	-
11	Menegazziaic acid	CH_3	O-CH_3	OH	-	-	-
13	Norstictic acid	CH_3	OH	CH-O	-	-	-
14	Fumarprotocetraric acid	-	-	-	O-CO-CH=CH-CO_2H	H	CH-O
17	Methylhypoprotocetraric	-	-	-	H	CH_3	CH_3
18	Usnic acid	-	-	-	-	-	-

Fig. 1. Ordination (PCoA) of the *Xanthoparmelia* specimens (white and grey symbols identify morphotypes M-I/M-IX from outcrops 1 and 2, respectively, according to *Table 1*) on the basis of the contents of depsidones quantified by UPLC-HDR-DAD. List of depsidones (**1-17**) in *Table 1*. Chemical groups of specimens (i-vi) are indicated according to the cluster analysis of *Fig. S2* in the Supporting Information. Magnified details of chemical groups iv and v are reported below the main diagram. Axis 1: 68.5% of variance; axis 2: 28.5% of variance.

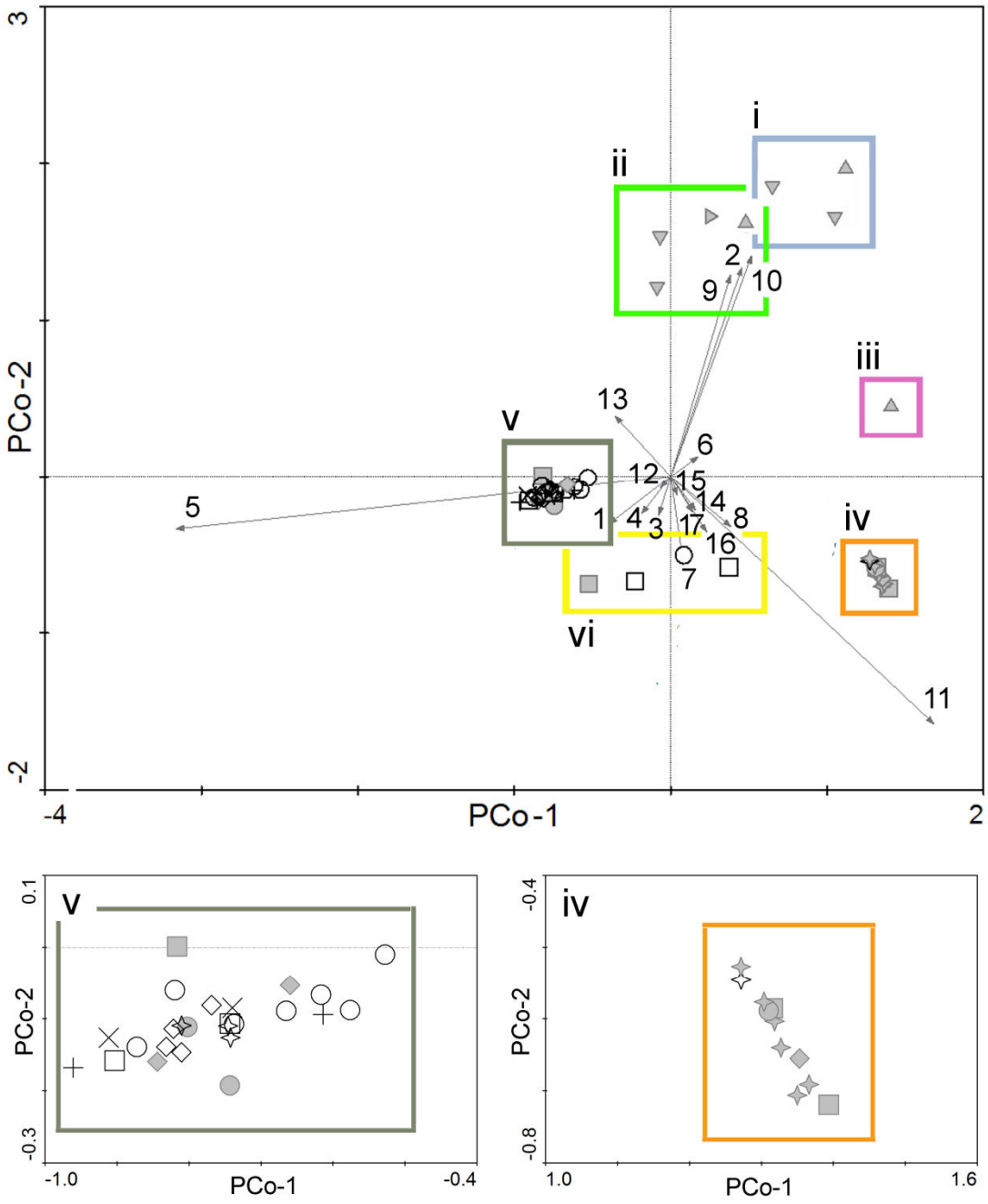

Fig. 2. Haplotype network describing the variability of the ITS region in the detected chemical groups (i-vi) of *Xanthoparmelia*. Respective haplotypes are identified with the letters A-P (47 sequences, 548 aligned bp, 59 variable sites, 56 parsimony informative sites, 16 unique haplotypes). Sizes of the circles reflect haplotype frequencies and are constructed with statistical parsimony as is implemented in TCS (each connecting line corresponds to one nucleotide difference). Colors in the circles identify the chemical patterns (i-vi) according to *Fig. 1* and *Fig. S2* in the Supporting Information. Three main haplotype groups (Hapl. gr.) are indicated according to major differences in their ITS sequences.

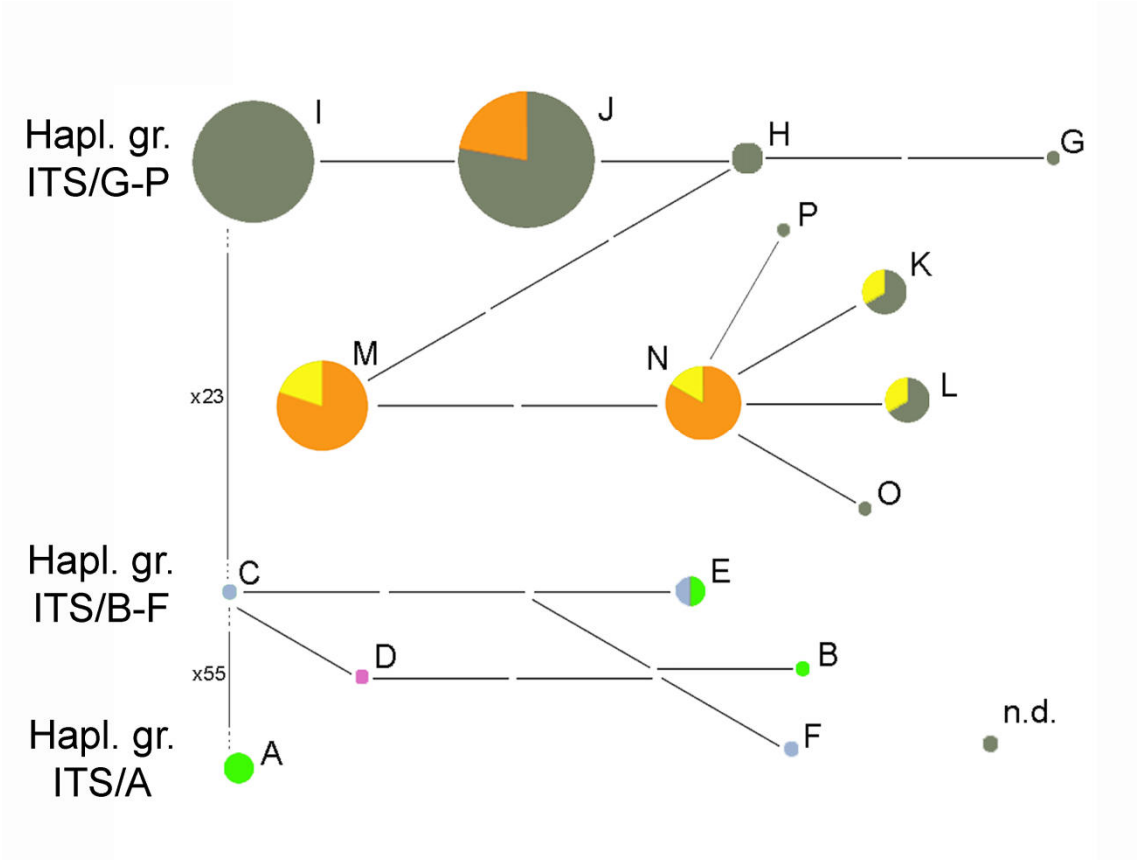

Fig. 3. Phylogenetic placement of fungal ITS sequences (505 bp aligned) of *Xanthoparmelia* specimens from outcrops 1 and 2 (colored circles identify the chemical patterns (i-vi) according to *Fig. 1* and *Fig. S2* in the Supporting Information; white and grey symbols identify morphotypes M-I/M-IX from outcrops 1 and 2, respectively, according to *Table 1*). Posterior probabilities (>0.70) are reported on the branches of the Bayesian tree, which includes sequences representative of a wide set of European and non-European *Xanthoparmelia* species (phenotypic characters in *Tables S1* and *S3*, respectively, in the Supporting Information).

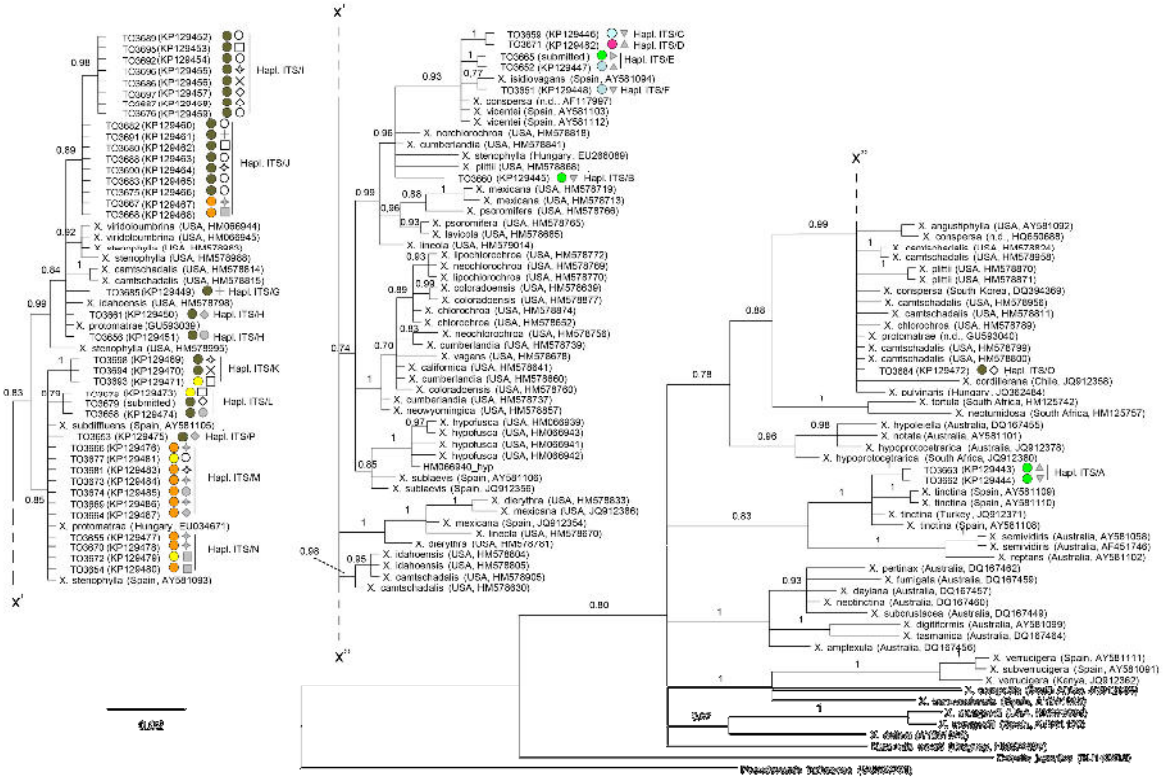

Entry for the Table of Contents